Journal of Combinatorial Optimization
https://doi.org/10.1007/s10878-021-00730-4

Regularized graph cuts based discrete tomography reconstruction methods

Marina Marčeta[1] · **Tibor Lukić**[1]

Accepted: 31 March 2021

Abstract
The topic of this paper includes graph cuts based computed tomography reconstruction methods in binary and multi-gray level cases. This approach combines the graph cuts and a gradient based method. The present paper introduces and analyses the shape circularity as a new regularization and incorporates it in a graph cuts based computed tomography reconstruction approach, thus introducing a new energy-minimization based reconstruction algorithm for binary tomography. Proposed method is capable for reconstructions in cases of limited projection view availability. Results of experimental evaluation of the considered graph cuts type reconstruction methods for both binary and multi-level tomography are presented.

Keywords Discrete tomography · Binary tomography · Shape circularity · Graph cuts optimization · Energy minimization methods

1 Introduction

Image reconstruction represents a collection of methods used to enhance and improve the quality of the image or to extract additional information from the image. Very often we need to obtain information about an object which is not visible or easily accessible. An area of image processing whose scope are these type of problems is named tomography.

Authors acknowledge the project "Innovative scientific and artistic research from the domain of the Faculty of Technical Sciences", grant no. 451 − 03 − 68/2020 − 14/200156.

✉ Marina Marčeta
marceta.marina@gmail.com

Tibor Lukić
tibor@uns.ac.rs

[1] Faculty of Technical Sciences, University of Novi Sad, Novi Sad, Serbia

Published online: 10 April 2021

Tomography deals with reconstructing images from the given projection data. Projection data is obtained by a wave penetrating through an unknown object. This wave is then detected on the opposite side of an object. A set of projection data is obtained at a particular angle. The source and detector are then rotated at a small angle, and a new projection is obtained. The object aimed to be restored is seen as a function with a domain that can be discrete or continuous and a range that is a given set of (usually) real numbers. *Discrete Tomography* (DT) (Herman and Kuba 1999, 2006) is a field of tomography that focuses on reconstruction of discrete images (finite number of pixel values) using much fewer number of projections. We distinguish binary tomography (BT) concentrating on binary images and multi-level discrete tomography concentrating on digital images that consist of numerous gray levels. DT has a wide range of applications in areas where the materials of the object under investigation are known before, such as industrial non-destructive testing or electron tomography, as well in many diagnostic approaches in medicine (Herman and Kuba 1999, 2006).

In the related conference publication (Marčeta and Lukić 2020), we proposed a new graph cuts based binary tomography reconstruction algorithm (GCORIENTBT) for limited projection availability. This approach incorporates the shape orientation (Žunić et al. 2006) as an a priori information about the solution into the reconstruction process.

This paper brings a new regularization approach based on the shape circularity (Žunić et al. 2010). We use the same graph cuts based optimization approach as in the case of the GCORIENTBT method, but, instead of the shape orientation, the shape circularity is reviewed and applied as an a priori information in the reconstruction process. We found the motivation for this choice in recently published paper (Lukić and Balázs 2020), where the circularity prior is successfully applied in a combination with convex-concave based regularization (Schüle et al. 2005). The proposed circularity based method (GCCIRCBT) has an important advantage compared to GCORIENTBT, since the gradient of the regularization is determined in an analytical way which makes the determination of the smooth solution fast by the SPG algorithm. Running time of the algorithm is significantly decreased compared to existing similar techniques. We demonstrate by experiments that the prior information can boost the performance of reconstruction in cases of very low number of projections. Additionally, this paper gives an overview and experimental evaluation of the most often used algorithms for multi-level tomography reconstruction problem, which, to the best of our knowledge was addressed by only few researches.

This paper is organized as follows. Section 2 gives a brief overview of the basic reconstruction problem. Section 3 begins by examining the approach that uses graph cuts for energy minimization, followed by the introduction of shape orientation and circularity as shape descriptors and finishing with describing and analyzing the new reconstruction method. Experimental results are provided in Sect. 4. Our conclusions are drawn in the final section.

2 Reconstruction problem

In this chapter we introduce some notations and define the DT problem mathematically.

DT reconstruction problem can be outlined by the following linear system of equations

$$\begin{aligned}
&a_{11}u_1 + a_{12}u_2 + a_{13}u_3 + \ldots + a_{1N}u_N = b_1\\
&a_{21}u_1 + a_{22}u_2 + a_{23}u_3 + \ldots + a_{2N}x_N = b_2\\
&a_{31}u_1 + a_{32}u_2 + a_{33}u_3 + \ldots + a_{3N}x_N = b_3\\
&\ldots\ldots\ldots\ldots\ldots\ldots\\
&a_{M1}u_1 + a_{M2}u_2 + a_{M3}u_3 + \ldots + a_{MN}x_N = b_M,
\end{aligned}$$

which we examine in its matrix form

$$A\,u = b, \tag{1}$$

where $A \in \mathbb{R}^{M\times N}$, $u \in \Lambda^N$, $b \in \mathbb{R}^M$ and $\Lambda = \{\lambda_1, \lambda_2, ..., \lambda_k\}$ for $k \geq 2$.

Unknown image to be reconstructed is denoted by u and is represented in a column vector form. Set Λ is given by the user and denotes the gray levels of the image, if $k = 2$, problem becomes problem of binary tomography. Matrix A is named *projection matrix*. Each row of this matrix is determined by one projection ray and its entries are calculated as the length of the intersection of the pixels and projection ray passing through them. The corresponding components of the vector b consist of the detected projection values calculated as a sum of products of the pixel's intensity and the corresponding length of the projection ray through that pixel.

Projection process is performed from different directions. For each projection direction a number of parallel projection rays is taken (parallel beam projection). The projection direction is determined by the angle α. Every two adjacent parallel projection rays are equidistant with their distance being equal to the side length of pixels. Number of parallel projection rays is specified in a way to cover the whole image grid.

The reconstruction problem means finding the solution image u of the linear system of equations (1), where the projection matrix A and the projection vector b are given. This system is often undetermined ($N > M$). We are interested in finding a reconstruction which resembles the original image as closely as possible, not just one that corresponds to the given projections. Therefore, it is necessary to use all available information (a priori information) about the object of interest in order to determine quality and acceptable solution.

3 Graph cuts reconstruction methods assisted by shape circularity and shape orientation

Image reconstruction is commonly performed by regularized energy minimization, due to its simplicity and generally good performance. In its most general setting one tries to recover a reconstructed version of the observed image y by minimizing an energy function which has the following form:

$$E(u) = F(Lu, b) + \lambda R(u). \tag{2}$$

An argument u^r which minimizes the energy function,

$$u^r = arg \min_u E(u) \tag{3}$$

is considered to be an estimate of the original image. The function F is called the data fidelity term and measures the distance between the data b and the reconstruction u after the forward operator L has acted on it. The function R is called the regularization term and it imposes a priori knowledge on the solution u. It is expected that small values of R will lead, up to a certain extent, to the elimination of the undesirable features. Regularization also provides numerical stabilization of image reconstruction problem. The regularization parameter λ controls the trade-off between the two terms, i.e. the level of smoothing vs. faithful recovery of the image detail.

3.1 Graph cut optimization

Graph cut optimization can be conveniently utilized to solve a wide variety image processing problems that can be formulated in terms of energy minimization (Boykov et al. 1998, 2001; Birchfield and Tomasi 1999; Kolmogorov and Zabih 2001; Kwatra et al. 2003; Boykov and Kolmogorov 2003; Boykov and Jolly 2001; Kim and Zabih 2003).

A directed, weighted graph $G = (X, \rho)$, is determined by a set of nodes X, that are connected together through edges ρ. All the edges are directed from one node to another and appointed some weight or cost. A cut of a graph G is a partition of set X into two disjoint subsets A named source and B named sink. Any cut determines a unique cut-set consisting of a set of edges that have one endpoint in each subset of the partition. Cost of a cut is calculated as a sum of weights of all edges going from A to B. The minimum cut problem consists of finding a cut with minimum cost among all possible cuts. Algorithms to solve this problem can be found in (Boykov and Kolmogorov 2004).

The main idea behind application of graph cuts method in energy minimization is construction of a graph specially designed for the energy function so that the solution of minimum cut problem also minimizes the energy function. The solution of the minimum cut problem, in turn, can be computed very efficiently by max-flow algorithms.

The Potts model in graph cuts theory, on which min-cut/max-flow algorithm is applied, is based on the minimization of the following energy

$$E(d) = \sum_{p \in \mathcal{P}} D(p, d_p) + \sum_{(p,q) \in \mathcal{N}} K_{(p,q)} \cdot (1 - \delta_{d_p, d_q}), \tag{4}$$

where $d = \{d_p | p \in \mathcal{P}\}$ represents the labelling of the image pixels $p \in \mathcal{P}$. By $D(p, d_p)$ we denote the data cost term, where $D(p, d_p)$ is a penalty or cost for assigning a label d_p to a pixel p. $K_{(p,q)}$ is an interaction potential between neighboring pairs p and q, $\mathcal{N}$ is a set of neighboring pairs. Function δ_{d_p, d_q} is a Kronecker delta function.

3.2 Geometric moments

The geometric moment of a digitized image u is defined by

$$m_{p,q}(u) = \sum_{(i,j)\in\Omega} u(i,j) i^p j^q,$$

where $\Omega \subseteq \mathbb{R}^2$ denotes the image domain.

The center of gravity (or centroid) of an image (or a shape) u is defined by

$$(C_x(u), C_y(u)) = \left(\frac{m_{1,0}(u)}{m_{0,0}(u)}, \frac{m_{0,1}(u)}{m_{0,0}(u)}\right).$$

The centroid enables the definition of the centralized moment which is translation invariant. The centralized moment of an image u of order $p+q$ is given by

$$\overline{m}_{p,q}(u) = \sum_{(i,j)\in\Omega} u(i,j)(i - C_x(u))^p (j - C_y(u))^q.$$

The shape is a characteristic of an object which allows numerical characterizations and, in addition, has high object discrimination capacity. Many approaches regarding shape descriptors have been developed (Sonka et al. 2007). There are shape descriptors that accurately describe specific shapes and the ones that describe single characteristics that are present over a variety of shapes. In this paper we will focus on two shape descriptors, namely orientation and circularity, and we will measure them using geometric moments.

3.3 Shape orientation

Shape orientation is determined by the angle α, which represents the slope of the axis of the second moment of inertia (orientation axis) of the considered shape (Sonka et al. 2007). The orientation (angle α) for the the given image u can be calculated by the following equation:

$$\frac{\sin(2\alpha)}{\cos(2\alpha)} = \frac{2 \cdot \bar{m}_{1,1}(u)}{\bar{m}_{2,0}(u) - \bar{m}_{0,2}(u)}. \tag{5}$$

Moments in (5) are translation invariant, making the orientation invariant to translation transformations, for more details see (Lukić and Balázs 2016; Žunić et al. 2006).

The graph cuts reconstruction method which applies the shape orientation in the binary tomography reconstruction process (GCORIENTBT) is proposed and analyzed in our recently published paper (Marčeta and Lukić 2020), therefore we omit its detailed description.

3.4 Shape circularity

Shape circularity is a familiar shape descriptor. Exploiting the fact that the circle has the largest area among all the shapes with the same perimeter, the most standard method defines the shape circularity $C_{st}(S)$ in the following way

$$C_{st}(S) = \frac{4\pi A(S)}{(P(S))^2}, \tag{6}$$

where $A(S)$ is the area of the shape S and $P(S)$ is the perimeter of S. It is easy to notice that $C_{st}(S)$ is not area based nor boundary based, since it uses the information both from the interior and boundary points.
For the given shape, represented by the image u, the circularity can also be rated or measured by the following formula

$$\mathcal{C}(u) = \frac{1}{2\pi(\mu_{2,0}(u) + \mu_{0,2}(u))}, \tag{7}$$

where $\mu_{p,q}(u)$ is the normalized moment of u of order $p+q$. It is defined by the following formula

$$\mu_{p,q}(u) = \frac{\overline{m}_{p,q}(u)}{m_{0,0}(u)^{1+\frac{p+q}{2}}}.$$

It is trivial to show, that the normalized moment, besides being translation invariant, is invariant to uniform scaling as well. The circularity measure $\mathcal{C}(u)$ is proposed and thoroughly analyzed in (Žunić et al. 2010). In addition, in the same paper it has been proven that circularity is highly performant in shape classification problems. The following Theorem summarizes the most important properties of $\mathcal{C}(u)$.

Theorem 1 *(Žunić et al. 2010) The circularity measure $\mathcal{C}(u)$, for a compact shape u (closed and bounded), satisfies:*

(a) $\mathcal{C}(u) \in (0, 1]$, *for all shapes defined by u;*
(b) $\mathcal{C}(u) = 1 \Leftrightarrow u$ *represents a circle;*
(c) $\mathcal{C}(u)$ *is invariant w.r.t. similarity transformations (translation, rotation and scaling);*
(d) For each $\delta > 0$ *there is a shape u such that* $0 < \mathcal{C}(u) < \delta$.

The standard circularity measure $C_{st}(S)$ penalizes deep intrusions into the shape, because such intrusions lead to an essential perimeter increase, which, by the definition, decreases $C_{st}(S)$. The measure $C(S)$ is area based and does not penalize such intrusions. On the other hand, $C(S)$ is robust to noise, as area based descriptor, whereas $C_{st}(S)$ can only cope with small levels of noise because it uses the shape perimeter for the computation. For our model we use $C(S)$ as a measure of circularity.

3.5 The new method based on shape circularity

Reconstruction method for solving discrete tomography problem we propose in this paper consists of two parts:

- Finding a continuous (smooth) solution of the energy minimization problem using gradient based minimization method. Information about the circularity of the original object is incorporated in the energy function.
- Discretization of the obtained smooth solution applying graph cuts based algorithm. Pixel values of the smooth image are used to define data cost term for the graph.

$$\min_{u\in[0,1]^N} E_Q(u) := w_P \|Au-b\|_2^2 + w_H \sum_{i=1}^{N}\sum_{j\in\Upsilon(i)} (u_i-u_j)^2 + \\ + w_C \left(\mathcal{C}(u)-\mathcal{C}^*\right)^2 + \mu\,\langle u, \tau-u\rangle\,, \tag{8}$$

Energy function we use for calculation of the smooth solution is given in the equation (8) and is constructed of four terms:

1. Data fitting term, $\|Au-b\|_2^2$, regularized by parameter $w_P > 0$. Data fitting term ensures adherence to the projection data.
2. Homogeneity term, $\sum_{i=1}^{N}\sum_{j\in\Upsilon(i)}(u_i-u_j)^2$, regularized by parameter $w_H > 0$. $\Upsilon(i)$ is set of indices of two neighbouring pixels (in x and y axis directions) of pixel i. This term ensures the smoothness of the solution.
3. Term, $(\mathcal{C}(u)-\mathcal{C}^*)^2$, measures the distance between the circularity of current solution($\mathcal{C}(u)$) and known circularity of the original image ($\mathcal{C}^*$). Parameter $w_C > 0$ determines the impact of the circularity regularization.
4. Concave regularization term, $\langle u, \tau-u\rangle$, where $\tau = [1, 1, \ldots, 1]^T$ is a vector of size N, has the role to move pixels intensities toward binary values. Influence of this term is gradually increased during the reconstruction and it is regulated by parameter $\mu > 0$.

Problem (8) is a constrained and quadratic type energy-minimization problem that can be solved by several optimization methods. We have selected Spectral Projected Gradient (SPG) optimization algorithm (Birgin et al. 2001) for this task, since it has shown good performance in successful application in similar problems (Lukić and Balázs 2016; Lukić and Nagy 2014; Nagy and Lukić 2016; Birgin et al. 2000). The SPG algorithm combines the non-monotone line search algorithm (Grippo et al. 1986) and the spectral gradient step-length selection (Barzilai and Borwein 1988; Raydan 1997; Birgin and Martínez 2001), its pseudo-code is presented in Alg. 1.

The gradient of the regularization term

$$\left(\mathcal{C}(u)-\mathcal{C}^*\right)^2$$

in the energy function (8) is determined in a fully analytical manner, for its exact expression see (Lukić and Balázs 2020). This allows a fast minimization process and

Algorithm 1: SPG optimization algorithm.

$u^0 = [0.5, 0.5, ..., 0.5]^T$;
$d^0 = P_\Omega(u^0 - \nabla E_Q(u^0)) - u^0$; $k = 0$;
repeat
  Determine the current step-length $\lambda^k > 0$ by a line search approach, see (Birgin et al. 2001);
  $u^{k+1} = u^k + \lambda^k d^k$;
  Calculate the gradient spectral step-length $\theta_{k+1} > 0$, see (Birgin et al. 2001);
  $d^{k+1} = P_\Omega(u^{k+1} - \theta_{k+1}\nabla E_Q(u^{k+1})) - u^{k+1}$; $k = k + 1$;
until $\|u^k - u^{k-1}\|_\infty < 10^{-2}$;
$u^{new} = u^k$;

determination of the smooth solution by SPG algorithm, in contrast to the GCORI-ENTBT method when the gradient of the shape orientation based regularization is calculated in numerical manner.

The stopping criterion for smooth solution is given by

$$\langle u, \tau - u \rangle < E_{bin},$$

where E_{bin} regulates the degree of binarization of the solution u and it is set to 100 in our experiments. Partial binarization of the continuous solution boosts the determination of data cost terms for graph cuts method.

Next action after calculation of the smooth solution is its full binarization. This is done by applying the graph cuts method based on the Potts model, described in Sect. 3.1. We construct energy function according to the one used in the Potts model (4) in the following way:

- Data cost term, D,

$$D(p, 0) = u(p),$$
$$D(p, 1) = 1 - u(p),$$

  where $u(p)$ represents the intensity of a pixel p.
- Set of neighboring pairs, $\mathcal{N}$,
  $(p, q) \in \mathcal{N}$ if the image coordinates of p and q differ for one value only.
- Interaction potential, K,

$$K_{(p,q)} = 1.$$

After successful construction of the energy function (4), the next task is solving a problem of finding a minimum of this function. That is achieved by implementing GCO graph cuts based optimization algorithm, introduced in (Boykov et al. 2001) and further analyzed in (Boykov and Kolmogorov 2004; Delong et al. 2010; Kolmogorov and Zabih 2004). The output of GCO algorithm are label values d_p for each pixel p, where d_p is predefined as $d_p = 0 \rightarrow 0$ and $d_p = 1 \rightarrow 1$. As a result of the adequate construction of the function (4), obtained label values determine intensities of pixels in the final (binary) solution, marking the end of the reconstruction process.

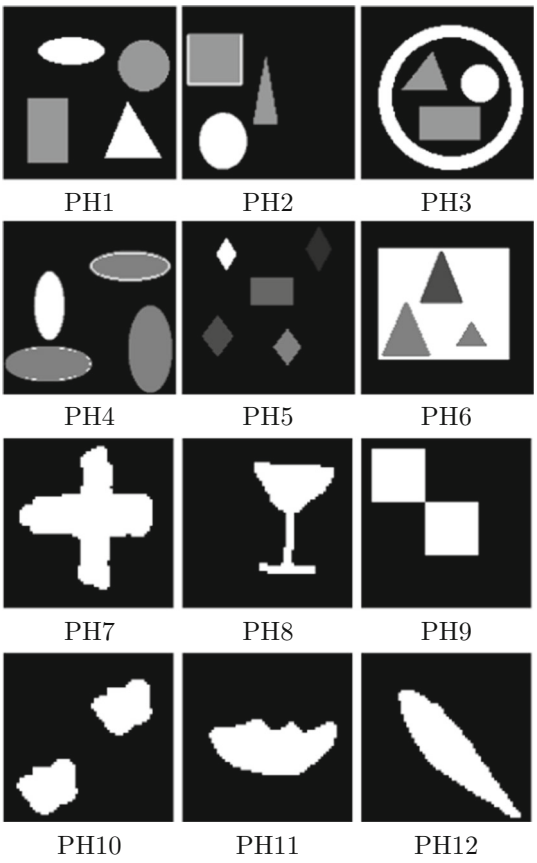

Fig. 1 Original test images. Phantoms PH1, PH2 and PH3 contain 3 different gray levels, PH4, PH5 and PH6 contain 6 different gray levels, while PH7, PH8, PH9, PH10, PH11, PH12 present binary images

We denote this method by Graph Cuts Binary Tomography Assisted by the Circularity prior (GCCIRCBT) reconstruction method.

4 Experimental results

In this section we aim to evaluate the performance of the algorithms that are, to the best of our knowledge, most commonly used for solving similar reconstruction problems in DT and to experimentally confirm if the new circularity prior improves the reconstruction quality. In order to achieve above mentioned goal, we use test set containing 12 test images (phantoms) presented in Fig. 1. PH1-3 contain 3 gray levels, PH4-6 contain 6 gray levels, while PH7-12 represent binary images. Images PH1-PH11 are synthetic, whereas PH12 is a binary segmented florescence image of Calcein stained Chinese hamster ovary cell. A total of 128 parallel rays is taken for each projection direction for multi gray level images and 64 projection rays for binary images. In all cases, the projection directions are uniformly selected between 0 and 180 degrees. This projection information is used as input in reconstruction algorithms:

Table 1 Experimental results for PH1, PH2 and PH3 images, using three different reconstruction methods. The abbreviation d indicates the number of projections.

d		PH1				PH2				PH3			
		6	9	12	15	6	9	12	15	6	9	12	15
MWP	(PE)	**255**	159	59	35	**143**	138	20	18	655	456	275	174
	(m.r. %)	**1.55**	0.97	0.36	0.21	**0.87**	0.84	0.12	0.11	3.99	2.78	1.67	1.06
TRDT	(PE)	412	175	48	28	209	141	17	17	412	301	101	41
	(m.r. %)	2.51	1.06	0.29	0.17	1.28	0.86	0.10	0.10	2.51	1.83	0.61	0.25
GCDT	(PE)	272	**69**	**8**	**5**	225	**124**	**12**	**12**	**272**	**116**	**20**	**9**
	(m.r. %)	1.66	**0.42**	**0.04**	**0.03**	1.37	**0.76**	**0.07**	**0.07**	**1.66**	**0.70**	**0.12**	**0.05**

The values representing the best performance are highlighted by bold font.

Table 2 Experimental results for PH1, PH2 and PH3 images, using three different reconstruction methods. The abbreviation e.t. means elapsed time in minutes and d indicates the number of projections.

d		PH1				PH2				PH3			
		6	9	12	15	6	9	12	15	6	9	12	15
MWPDT	(PRE)	**14.70**	12.19	9.96	9.08	**14.11**	**18.94**	6.08	7.71	**19.83**	18.77	18.80	16.43
	(e.t.)	1.76	2.63	3.17	4.06	5.34	8.17	6.36	11.62	2.19	2.87	4.30	4.66
TRDT	(PRE)	18.66	14.72	10.61	8.87	17.98	17.30	7.09	7.09	23.64	17.87	13.66	10.61
	(e.t.)	7.73	12.58	14.55	17.77	6.24	10.82	16.01	17.74	7.28	11.07	13.39	16.00
GCDT	(PRE)	23.24	**11.12**	**6.52**	**4.39**	26.77	21.04	**6.01**	**6.00**	25.87	**14.96**	**7.59**	**5.60**
	(e.t.)	7.73	12.58	14.55	17.77	6.25	10.82	16.01	17.74	7.29	11.07	13.40	16.01

The values representing the best performance are highlighted by bold font.

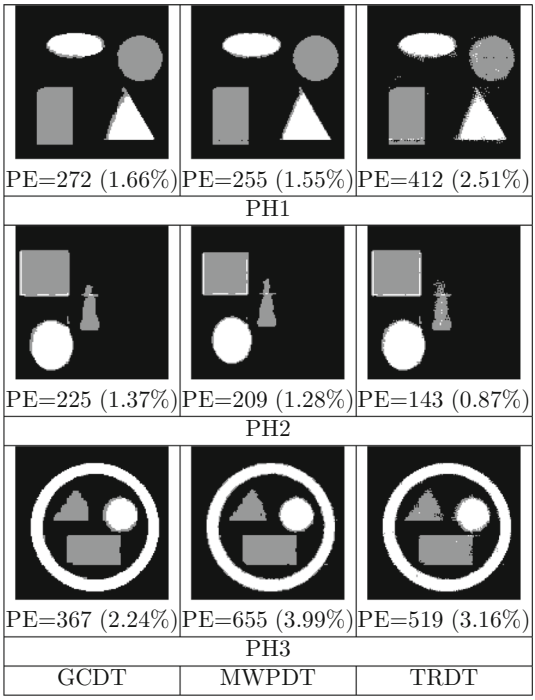

Fig. 2 Reconstructions of the 3 gray level test images using data from 6 projection directions

- Graph Cuts Discrete Tomography Algorithm (GCDT) (Lukić and Marčeta 2017)
- Discrete Algebraic Reconstruction Technique (DART) (Batenburg and Sijbers 2007)
- Method based on classical threshold (TRDT)
- Multi Well Potential based method (MWPDT) (Lukić 2011)
- Graph Cuts Tomography Assisted by the Orientation prior (GCORIENTBT) (Marčeta and Lukić 2020)
- Graph Cuts Binary Tomography Assisted by the Circularity prior (GCCIRCBT), introduced in this paper

MWPDT method is developed and used only for phantoms with 3 gray levels, GCORIENTBT and GCCIRCBT only for binary images, while the rest of the algorithms mentioned in this section can be used for reconstruction of images with arbitrary number of gray levels. In our experiments, each reconstruction method (GCDT, DART, TRDT, MWPDT, GCORIENTBT, GCCIRCBT) is completely implemented in programming language Matlab.

In the evaluation process, we analyze the quality of the reconstructions. The quality of the reconstructions is expressed by the pixel error (PE), i.e. the absolute number of the misclassified pixels, and by the misclassification rate ($m.r.$), i.e. the pixel error measure relative to the total number of image pixels. Additionally, as a qualitative error measure, we consider the projection error, defined by $PRE = \|Au^r - b\|$, where u^r represents the reconstructed image. This error indicates the accordance of the reconstruction with the given projection data.

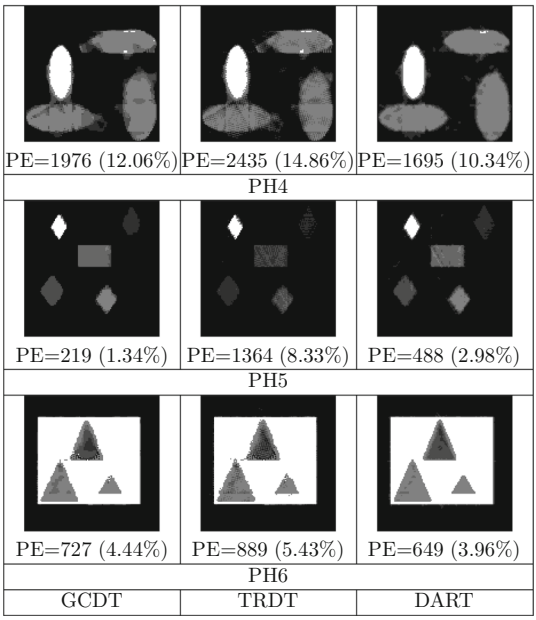

Fig. 3 Reconstructions of the 6 gray level test images using data from 6 projection directions

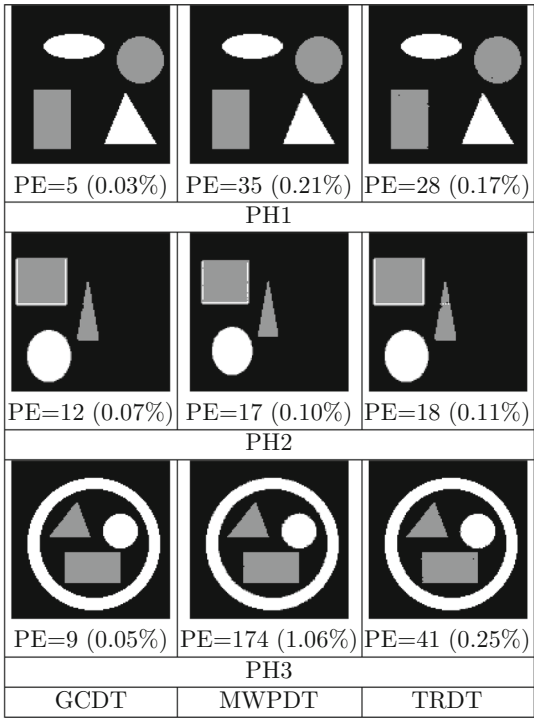

Fig. 4 Reconstructions of the 3 gray level test images using data from 15 projection directions

Table 3 Experimental results for PH4, PH5 and PH6 images, using three different reconstruction methods. The abbreviation d indicates the number of projections.

d		PH4				PH5				PH6			
		6	9	12	15	6	9	12	15	6	9	12	15
GCDT	(PE)	1976	**804**	**551**	**399**	**219**	**134**	**42**	**28**	727	**473**	**251**	**192**
	(m.r. %)	12.06	**4.91**	**3.36**	**2.44**	**1.34**	**0.82**	**0.26**	**0.17**	4.44	**2.89**	**1.53**	**1.17**
TRDT	(PE)	2435	1415	1188	998	1364	1330	1286	1274	889	807	587	552
	(m.r. %)	14.86	8.64	7.25	6.09	8.32	8.12	7.85	7.78	5.43	4.92	3.58	3.37
DART	(PE)	**1695**	1242	1177	1089	488	379	288	319	**649**	836	596	707
	(m.r. %)	**10.34**	7.58	7.18	6.65	2.98	2.31	1.76	1.95	**3.96**	5.10	3.64	4.32

The values representing the best performance are highlighted by bold font.

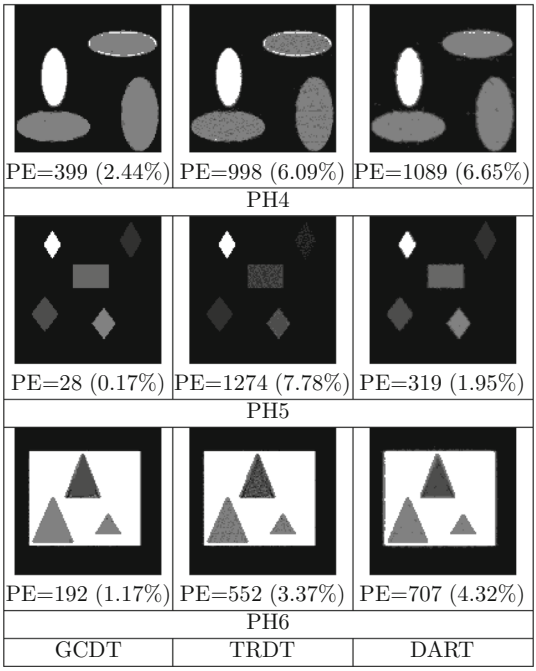

Fig. 5 Reconstructions of the 6 gray levels test images using data from 15 projection directions

We compare performance of the observed algorithms on the various projection data of the test images. The projection direction is determined by the angle α and, in this section, number of different projection angles used for obtaining projection data is denoted by d. Horizontal and vertical projection data provide enough information for determination of circularity and orientation shape descriptors (see Lukić and Balázs 2020). Thus, orientation and circularity of a shape do not present any additional information about an object if horizontal and vertical projection data is known. Therefore, in cases of 3 or more projection angles circulation and orientation as a priori information are redundant, as they are already present in projection values. This is the reason why for reconstructions that use higher number of projections, we do not show results for GCORIENTBT and GCCIRCBBT (they would be identical to those obtained by GCDT).

Results regarding the performance of different algorithms on test images PH1, PH2 and PH3 (Tables 1, 2 and Figs. 2, 4), show that for PE and $m.r.$ as metrics, method GCDT provided the best results in 10 out of 12 cases, for PRE metric GCDT method dominates in 8 cases, while in terms of the execution time MWPDT method prevails. GCDT uses significantly higher number of iterations for obtaining the smooth solution compared to MWPDT method in total, thus resulting in greater consumption of time.

Reconstruction results of phantoms with 6 different gray levels (Table 3) show that, compared to TRDT and DART, GCDT method prevails in 10 out of 12 cases, whilst DART performs the best in 2 cases. In Figs. 3, 5 reconstructions from 6 and 15 projection directions respectively are presented.

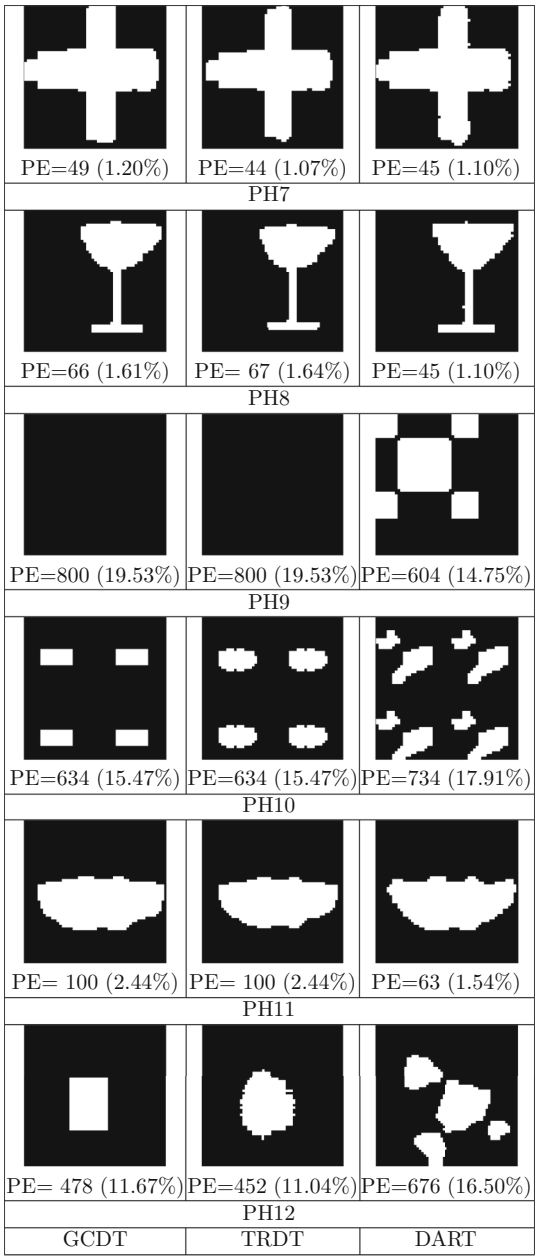

Fig. 6 Reconstructions of the binary test images using data from 2 projection directions (vertical and horizontal)

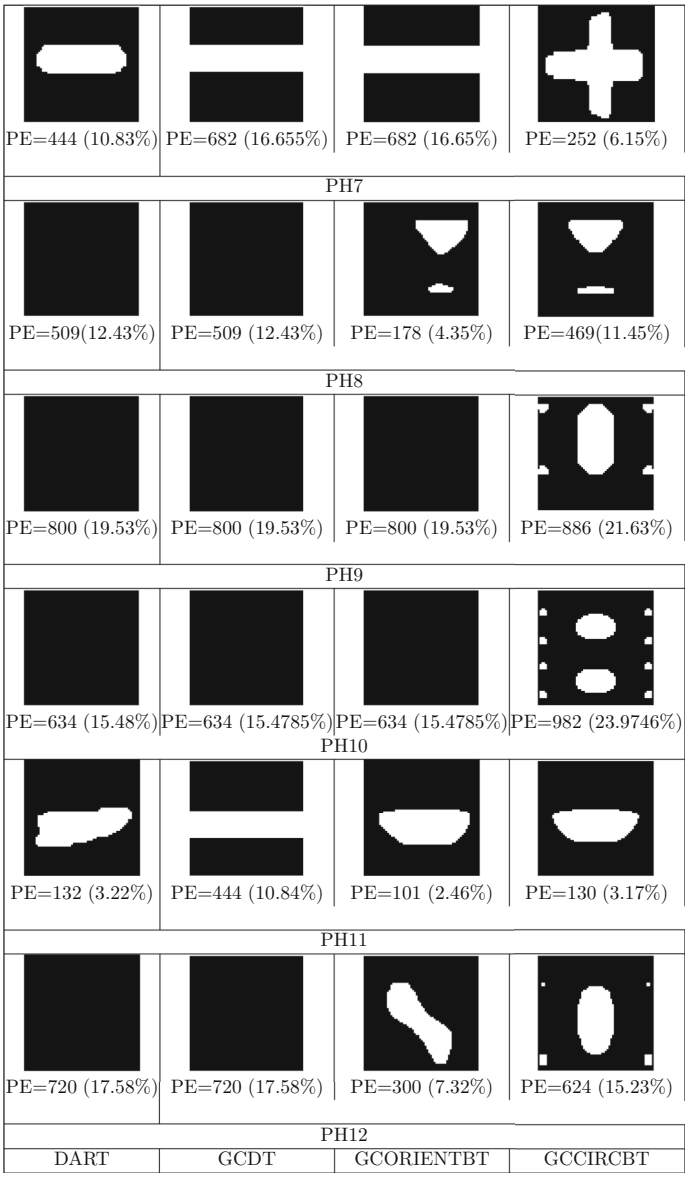

Fig. 7 Reconstructions of the binary test images using data from 1 projection direction, $\alpha = 0°$

Results down to this point of the analysis show competitive performance of a model based on the combination of graph cuts and a gradient based method (GCDT). This encourages us to test and develop this algorithm further.

Our experiments on binary images (Fig. 6) demonstrate that GCDT method gives poor results in cases of the reconstruction from two projections. In order to avoid this drawback we can add orientation and circularity as a priori information to GCDT

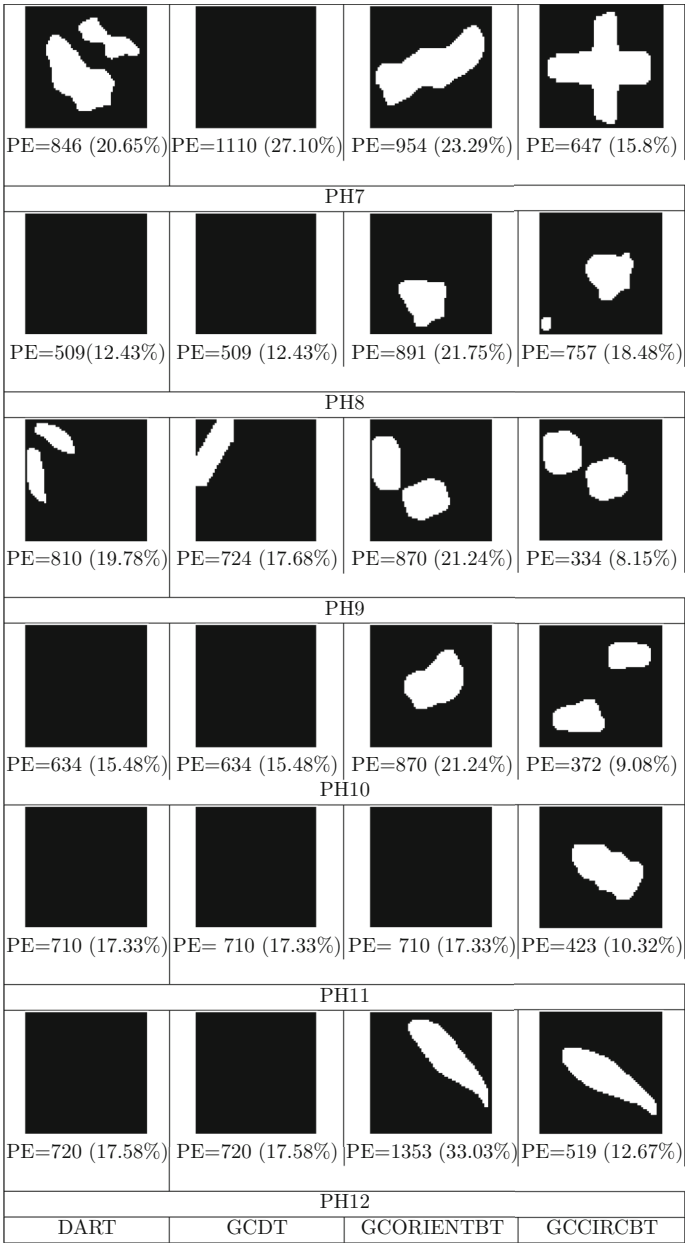

Fig. 8 Reconstructions of the binary test images using data from 1 projection direction, direction angle is $\alpha = 60^\circ$

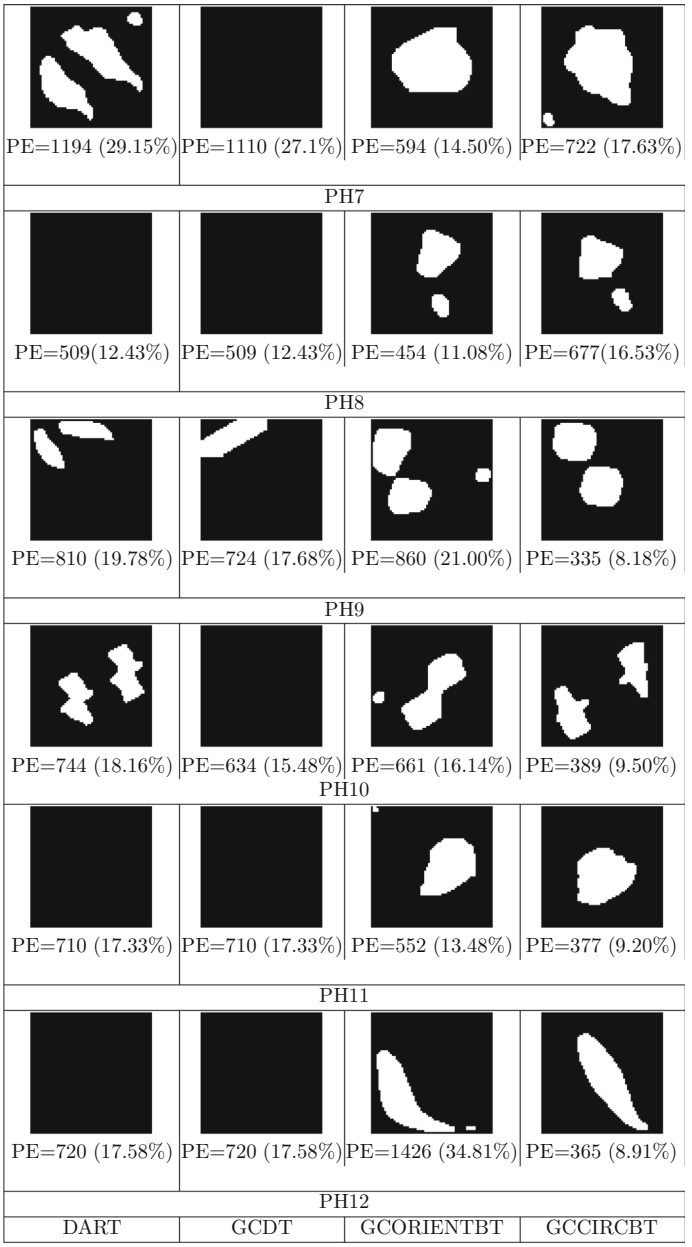

Fig. 9 Reconstructions of the binary test images using data from 1 projection direction, direction angle is $\alpha = 30°$

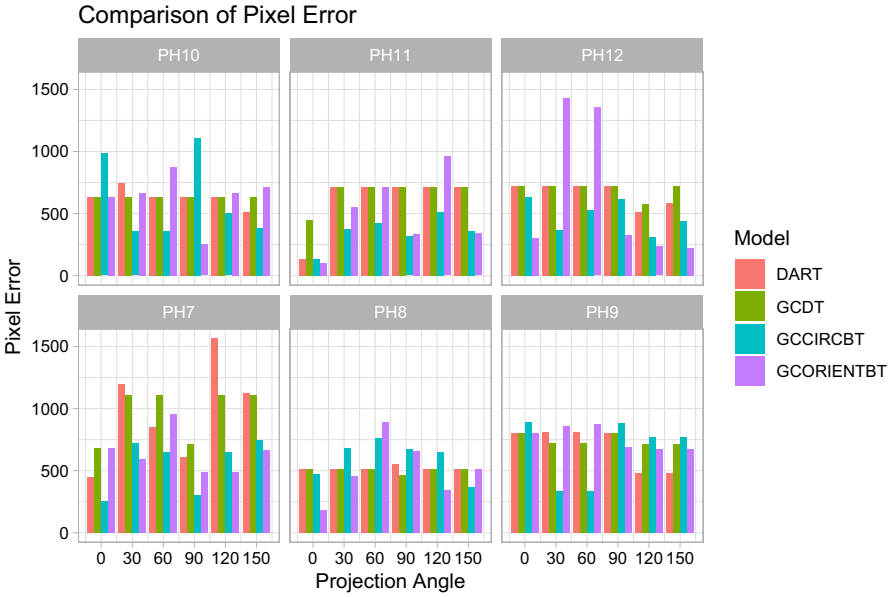

Fig. 10 Experimental results for BT using four different reconstruction methods (Pixel Error)

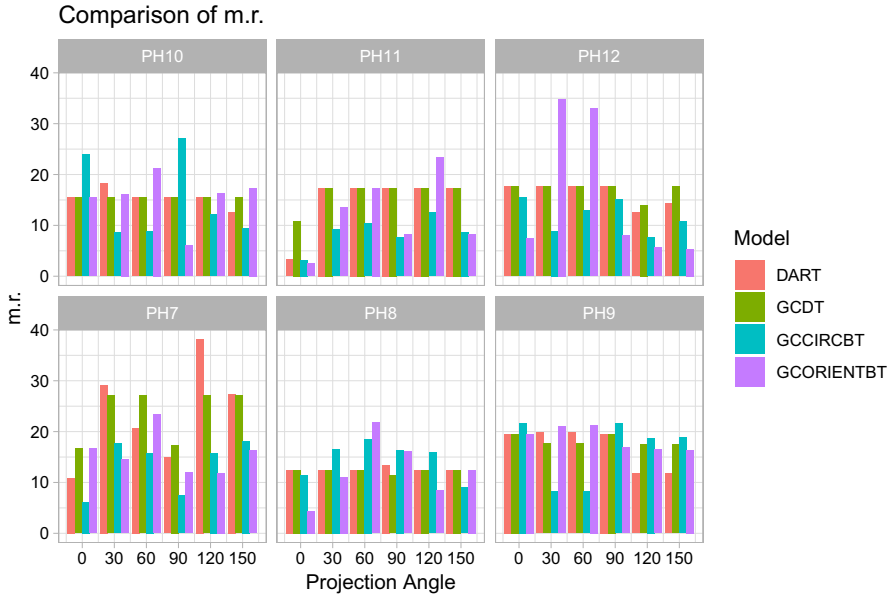

Fig. 11 Experimental results for BT using four different reconstruction methods (m.r.)

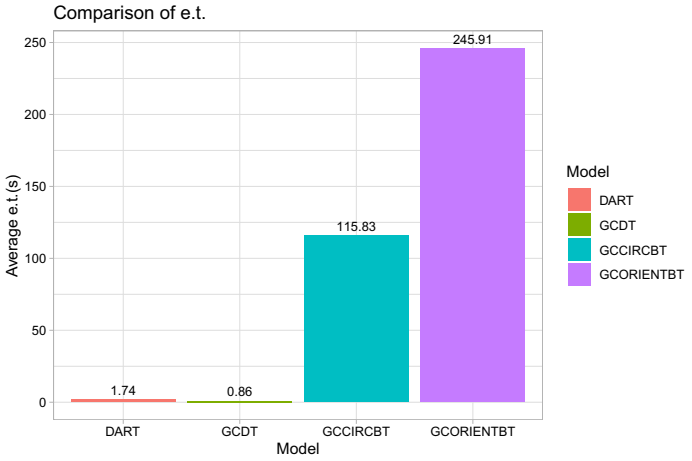

Fig. 12 Experimental results for BT using four different reconstruction methods (average e.t.)

method, thus building the GCORIENTBT and GCCIRCBT algorithm. Later, we have compared these algorithms with two other reconstruction methods (DART, GCDT) (Figs. 10, 11). For analyzis we have used 6 binary images, data was given from one projection, and we have tested the model by using 6 different projection angles.

In (Marčeta and Lukić 2020) it was shown that GCORIENTBT gives very good results in cases of limited projection view availability. We have now been inquiring if the circularity is equally good or even better to use as a regularization term. In 17 out of 36 cases GCCIRCBT gives the best reconstruction (smallest PE/m.r.) and GCORIENTBT wins in 13 cases. It can be noticed that, as expected, by adding the prior to GCDT method, significantly better results for BT are obtained in cases of limited projection data availability. The noticeable advantage of GCCIRCBT is in running time, execution time of GCCIRCBT is in most of the cases significantly shorter compared to its best competitor GCORIENTBT (Fig. 12).

Summarizing the results obtained by the total of 24 multi-gray level analyzed reconstruction tasks, see Tables 1 and 3, the quality of the reconstruction, indicated by m.r. for the proposed GCDT method was the best in 20 cases, i.e. in 83% of the analyzed cases. Further, GCORIENTBT and GCCIRCBT together performed better in 83% of the cases, with GCCIRCBT being slightly superior, thus indicating excellent performance of graph cuts based reconstruction approach in DT as well as prevailing advantages of using shape circularity as an a priori information.

5 Conclusions

This paper has highlighted the noteworthy performance of an algorithm based on the combination of gradient based method and graph cuts optimization method for solving problems in Discrete Tomography. In cases of very limited projection accessibility we modified the method using shape descriptor circularity as an a priori information

about the object. Conducted experiments gave priority in reconstruction quality to the proposed method compared to the formerly published reconstruction methods. In conclusion, our results show that it is suitable to use the combination of a gradient based method with the graph cuts optimization method, which can be successfully enhanced by circularity as an a priori information, for providing high quality reconstructions in discrete tomography.

Data availability The data (digital test images) that support the findings of this study are available from the corresponding author, upon reasonable request.

Declarations

Conflict of interest The authors declare that there is no conflict of interest.

Funding The research is not financially supported.

Code availability The Matlab code used in this paper is available on request per email from the corresponding author.

References

Barzilai J, Borwein JM (1988) Two point step size gradient methods. IMA J Num Anal 8:141–148
Batenburg KJ, Sijbers J (2007) DART: A Fast heuristic algebraic reconstruction algorithm for discrete tomography. In Proceedings of International conference on image processing (ICIP), pages 133–136
Birchfield S, Tomasi C (1999) Multiway cut for stereo and motion with slanted surfaces. Proc. International Conf. Computer Vision, pages 489–495
Birgin E, Martínez J (2001) Spectral conjugate gradient method for unconstrained optimization. Appl Math Optim 43:117–128
Birgin E, Martínez J, Raydan M (2000) Nonmonotone spectral projected gradient methods on convex sets. SIAM J Optim 10:1196–1211
Birgin EG, Martínez JM, Raydan M (2001) Algorithm: 813: SPG - software for convex-constrained optimization. ACM Trans Math Softw 27:340–349
Boykov Y, Jolly MP (2001) Interactive graph cuts for optimal boundary and region segmentation of objects in N-D images. In Proc. International Conf. Computer Vision, pages 105–112
Boykov Y, Kolmogorov V (2003) Computing geodesics and minimal surfaces via graph cuts. In Proc. International Conf. Computer Vision, pages 26–33
Boykov Y, Kolmogorov V (2004) An experimental comparison of min-cut/max-flow algorithms for energy minimization in vision. IEEE Trans. PAMI 26(9):1124–1137
Boykov Y, Veksler O, Zabih R (1998) Markov random fields with efficient approximations. In Proceedings of IEEE Conf. Computer Vision and Pattern Recognition, pages 648–655
Boykov Y, Veksler O, Zabih R (2001) Fast approximate energy minimization via graph cuts. IEEE Trans PAMI 23(11):1222–1239
Delong A, Osokin A, Isack H. N, Boykov Y (2010) Fast approximate energy minimization with label costs. Proc. IEEE Conf. computer vision and pattern recognition 96(1):1–27
Grippo L, Lampariello F, Lucidi S (1986) A nonmonotone line search technique for Newton's method. SIAM J Numer Anal 23:707–716
Herman GT, Kuba A (1999) Discrete tomography: foundations, algorithms and applications. Birkhäuser
Herman GT, Kuba A (2006) Advances in discrete tomography and its applications. Birkhäuser
Kim J, Zabih R (2003) Automatic segmentation of contrast- enhanced image sequences. In Proc. International Conf. Computer Vision, pages 502–509
Kolmogorov V, Zabih R (2001) Visual correspondence with occlusions using graph cuts. In Proc. International Conf. Computer Vision, pages 508–515

Kolmogorov V, Zabih R (2004) What energy functions can be minimized via graph cuts? IEEE Trans PAMI 26(2):147–159

Kwatra V, Schoedl A, Essa I, Turk G, Bobick A (2003) Graphcut textures: image and video synthesis using graph cuts. In Proc. SIGGRAPH 2003, pages 277–286. ACM Trans. Graphics

Lukić T (2011) Discrete tomography reconstruction based on the multi-well potential. In Proceedings of combinatorial image analysis - 14th international workshop (IWCIA), volume 6636 of *LNCS*, pages 335–345, Madrid, Spain. Springer-Verlag

Lukić T, Balázs P (2016) Binary tomography reconstruction based on shape orientation. Pattern Recognit Lett 79:18–24

Lukić T, Balázs P (2020) Shape circularity assisted tomography reconstruction. Physica Scripta 95(10):105211

Lukić T, Marčeta M (2017) Gradient and graph cuts based method for multi-level discrete tomography. In Proceedings of combinatorial image analysis - 18th International workshop (IWCIA), LNCS, pages 322–333, Plovdiv, Bulgaria, Springer-Verlag

Lukić T, Nagy B (2014) Deterministic discrete tomography reconstruction method for images on triangular grid. Pattern Recognit Lett 49:11–16

Marčeta M, Lukić T (2020) Graph cuts based tomography enhanced by shape orientation. In T. Lukic, R. P. Barneva, V. E. Brimkov, L. Comic, and N. Sladoje, editors, Combinatorial image analysis - 20th International workshop, IWCIA 2020, Novi Sad, Serbia, July 16-18, 2020, Proceedings, volume 12148 of lecture notes in computer science, pages 219–235. Springer. https://doi.org/10.1007/978-3-030-51002-2_16

Nagy B, Lukić T (2016) Dense projection tomography on the triangular tiling. Fundamenta Informaticae 145:125–141

Raydan M (1997) The Barzilai and Browein gradient method for the large scale unconstrained minimization problem. SIAM J Optim 7:26–33

Schüle T, Schnörr C, Weber S, Hornegger J (2005) Discrete tomography by convex-concave regularization and D.C. programming. Discrete Appl Math 151:229–243

Sonka M, Hlavac V, Boyle R (2007) Image processing, analysis, and machine vision. Thomosn-Engineering

Žunić J, Rosin PL, Kopanja L (2006) On the orientability of shapes. IEEE Trans Image Process 15:3478–3487

Žunić J, Hirota K, Rosin PL (2010) A hu invariant as a shape circularity measure. Pattern Recognit 43:47–57